LETTER

doi:10.1038/nature11728

Ultrahard nanotwinned cubic boron nitride

Yongjun Tian[1], Bo Xu[1], Dongli Yu[1], Yanming Ma[2], Yanbin Wang[3], Yingbing Jiang[4], Wentao Hu[1], Chengchun Tang[5], Yufei Gao[1], Kun Luo[1], Zhisheng Zhao[1], Li-Min Wang[1], Bin Wen[1], Julong He[1] & Zhongyuan Liu[1]

Cubic boron nitride (cBN) is a well known superhard material that has a wide range of industrial applications. Nanostructuring of cBN is an effective way to improve its hardness by virtue of the Hall–Petch effect—the tendency for hardness to increase with decreasing grain size[1,2]. Polycrystalline cBN materials are often synthesized by using the martensitic transformation of a graphite-like BN precursor, in which high pressures and temperatures lead to puckering of the BN layers[3]. Such approaches have led to synthetic polycrystalline cBN having grain sizes as small as ~14 nm (refs 1, 2, 4, 5). Here we report the formation of cBN with a nanostructure dominated by fine twin domains of average thickness ~3.8 nm. This nanotwinned cBN was synthesized from specially prepared BN precursor nanoparticles possessing onion-like nested structures with intrinsically puckered BN layers and numerous stacking faults. The resulting nanotwinned cBN bulk samples are optically transparent with a striking combination of physical properties: an extremely high Vickers hardness (exceeding 100 GPa, the optimal hardness of synthetic diamond), a high oxidization temperature (~1,294 °C) and a large fracture toughness (>12 MPa $m^{1/2}$, well beyond the toughness of commercial cemented tungsten carbide, ~10 MPa $m^{1/2}$). We show that hardening of cBN is continuous with decreasing twin thickness down to the smallest sizes investigated, contrasting with the expected reverse Hall–Petch effect below a critical grain size or the twin thickness of ~10–15 nm found in metals and alloys.

Polycrystalline cubic boron nitride possesses high hardness and high chemical stability and is the best-known material for cutting ferrous and carbide-forming hard substances where diamond completely fails. However, commercial polycrystalline cBNs have grain sizes in the micrometre scale and a Vickers hardness (H_V) of only 33–45 GPa (refs 6, 7), much lower than that of diamond (~100 GPa)[8]. The application of cBN is therefore limited. For decades, scientists have designed various ways to increase the hardness of polycrystalline cBN[1,2,4,5] while retaining its excellent chemical stability.

The Hall–Petch effect[9,10], through which material hardness increases with decreasing grain size, has been widely observed. For polycrystalline cBN or diamond, reducing the grain size has been the most widely used approach for enhancing hardness. Conditions of high pressure and high temperature (HPHT) are required for the synthesis because temperature enhances the nucleation rate, and pressure suppresses grain growth by reducing the atomic diffusion responsible for crystallization[2,11]. Experimentally, nanograined (ng) diamonds with grain sizes of 10–30 nm have been synthesized[11]. High Knoop hardnesses of up to 110–140 GPa have been reported. Efforts in reducing the grain size further to below 10 nm have been unsuccessful as a result of intergranular fractures in these bulk ng-diamonds[12]. For cBN, the best attempts[1,2] performed so far have produced ng-cBN samples at pressures ~20 GPa with a minimum grain size of 14 nm and a record hardness of 85 GPa. This grain size is close to the critical value at which the Hall–Petch relation breaks down, as demonstrated in metals and alloys[13–16]. It remains a technical challenge to synthesize polycrystalline cBNs with perfect grain boundaries and smaller grain sizes, because numerous high-energy grain boundaries in a polycrystalline material generate large driving forces for grain growth.

Fine twin domains can be stabilized within materials capable of twinning. Coherent twin boundaries possess excess energy that is typically about one order of magnitude lower than that of grain boundaries[15]. This makes nanotwinned structures energetically more stable than their nanograined counterparts, thereby allowing finer control of domain size. Twin boundaries have been experimentally verified to have a hardening effect identical to that of high-angle grain boundaries[15], because, similarly to grain boundaries, twin boundaries also serve as barriers against gliding dislocations. Hence, the synthesis of nanotwinned substructures within grains may be a feasible route to achieving ultrafine microstructural sizes approaching a few nanometres. In practice, however, a strategically designed experimental protocol essential to fine-tune nanotwin substructures has yet to be achieved.

The use of graphite-like BN as precursors merely generates ng-cBN[1,2,4,5], although twin domains are occasionally observed during the growth of cBN single crystals as undesired defects[17,18]. Here we report the synthesis of ubiquitously nanotwinned cBN (nt-cBN) with an average twin thickness of 3.8 nm under HPHT conditions, using a special turbostratic onion-like BN (oBN) nanoparticle precursor material.

The starting oBN nanoparticles (~30–150 nm in diameter) consisted of concentric BN spherical shells (Fig. 1a, b) with abundant puckering and stacking faults. The inter-shell spacing was determined by X-ray diffraction at 0.351 nm (Supplementary Fig. 2a), which is slightly larger than the inter-layer spacings in hexagonal (0.3328 nm) and rhombohedral (0.334 nm) BN[17]. The oBN precursors were pressed into a pellet (2.5 mm in diameter and 1 mm in height) and subjected to HPHT treatments with a multi-anvil apparatus. X-ray diffraction and Raman spectroscopy were performed on the recovered samples to characterize structural phase transformations (Supplementary Fig. 2). At 15 GPa, no transformation was observed at temperatures below 1,000 °C. Transformation into a translucent cubic phase mixed with a small amount of the wurtzite phase occurred above 1,200 °C. The sample transformed entirely into transparent cBN (Fig. 1c and Supplementary Fig. 1) above 1,600 °C. Other synthetic trials performed at different pressures from 12 GPa to 25 GPa showed a similar temperature dependence of the phase transformation. For comparison, a considerably higher temperature (2,200 °C) was used to acquire pure cBN when graphite-like BN precursors were employed[1]. The use of the oBN precursor is responsible for the significantly reduced synthetic temperature (by about 600 °C) and the stabilization of nanotwinned microstructure (see below).

The synthetic nt-cBN bulk samples had a diameter of about 2 mm and possessed a unique homogeneous microstructure. Typical transmission electron microscopy (TEM) and high-resolution TEM (HRTEM) images of an as-synthesized bulk sample are shown in Fig. 1d–f. Grains were about the same size as the original onions, irregular in shape but approximately equiaxed. Selected area electron diffraction (inset of Fig. 1d) confirmed that the sample was pure cBN containing randomly oriented nanograins. HRTEM revealed a high

[1]State Key Laboratory of Metastable Materials Science and Technology, Yanshan University, Qinhuangdao 066004, China. [2]State Key Laboratory for Superhard Materials, Jilin University, Changchun 130012, China. [3]Center for Advanced Radiation Sources, University of Chicago, Chicago, Illinois 60439, USA. [4]TEM Laboratory, University of New Mexico, Albuquerque, New Mexico 87131, USA. [5]School of Material Science and Engineering, Hebei University of Technology, Tianjin 300130, China.

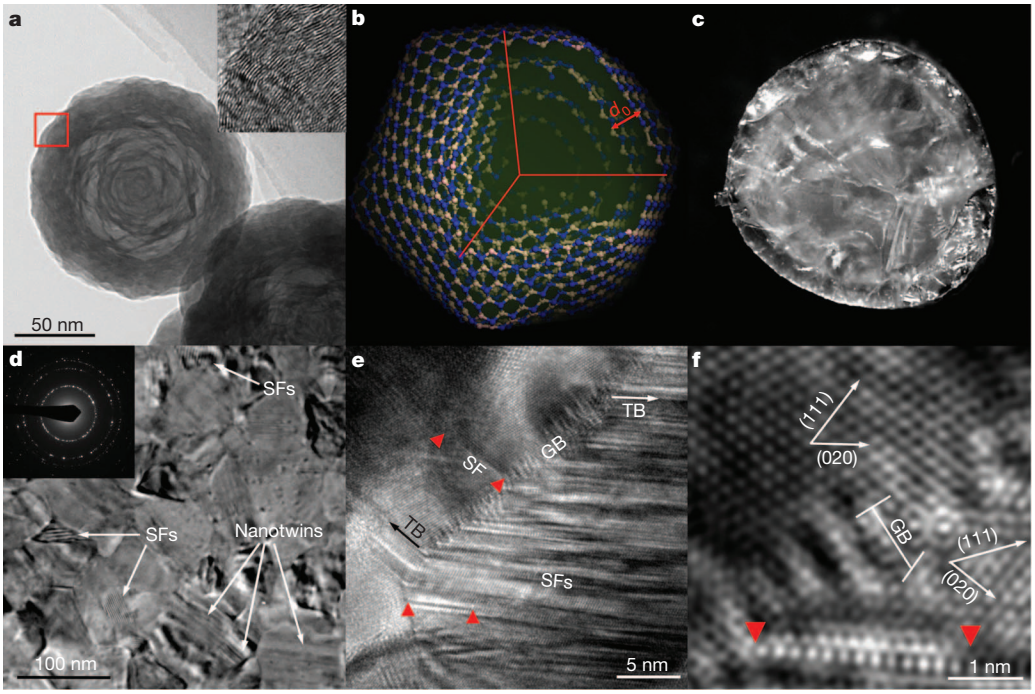

Figure 1 | Starting oBN nanoparticles and nt-cBN bulk synthesized at 15 GPa and 1,800 °C. **a**, TEM image of oBN nanoparticles. Inset, HRTEM image corresponding to the position marked with the red box, showing defects including lattice puckering, bending and stacking faults. **b**, Schematic icosahedral model of a five-shell oBN nanoparticle. d_0 is the inter-shell spacing. **c**, Photograph of an nt-cBN bulk sample with a diameter of about 2 mm. **d**, TEM image of a typical microstructure in nt-cBN. Nanotwins and stacking faults (SFs) are marked. Inset, a selected area electron diffraction pattern. **e**, HRTEM image of nt-cBN showing Shockley partial dislocations (red triangles) emitted from grain boundaries (GB) and a high density of stacking faults in twin domains. TB, twin boundary. **f**, Enlarged HRTEM image of **e**, showing the orientation relationship between adjacent nanograins.

density of dislocations at grain boundaries, as well as a high density of stacking faults within the twin domains. Narrow and sharp high-angle grain boundaries about five or six atomic layers thick were frequently present (Fig. 1e, f). All nanograins contained densely spaced lamellar {111} twins (Fig. 2a, b). Figure 2c depicts the twin-thickness distribution derived from 726 counts of 60 grains based on TEM and HRTEM images. Twin thicknesses were predominantly below 10 nm, with an average of 3.8 nm. As a result of the low excess energy of twin boundaries, variations in duration (from several minutes to half an hour) during the HPHT treatments did not noticeably affect the average and distribution of twin thickness, indicating that the nanotwins are highly stable.

The H_V of bulk nt-cBN samples was measured with a standard square-pyramidal diamond indenter. Reliable hardness values are best determined from the asymptotic hardness region through a well-controlled indentation process[19,20]. We recorded the variations in H_V with respect to a series of applied loads (Fig. 3). The asymptotic hardness obtained at loads above 3 N reached an extremely high value of 108 GPa, which is the highest hardness reported so far for polycrystalline cBN and exceeds even that of synthetic diamond. Overall, the hardness measured for different nt-cBN samples synthesized between 1,800 and 1,950 °C at 12–15 GPa ranged from 95 GPa to 108 GPa. For direct comparison, we measured the hardness of commercial cBN single crystals with the same technique and obtained values lower than 49 GPa with loads of up to 4.9 N, above which the crystals fractured. The results are in good agreement with other reported hardness data (30–43 GPa) on cBN single crystals[21]. Our measured Knoop and nanoindentation hardnesses of nt-cBN samples are 77.7 and 98.5 GPa (Supplementary Table 1), respectively.

Radial cracks formed in bulk nt-cBN at loads of 9.8 and 19.6 N were used to determine the fracture toughness (K_{IC}) with the equation[22] $K_{IC} = 7.42 \times 10^{-2} F/L^{1.5}$, where L and F are the length of the crack and

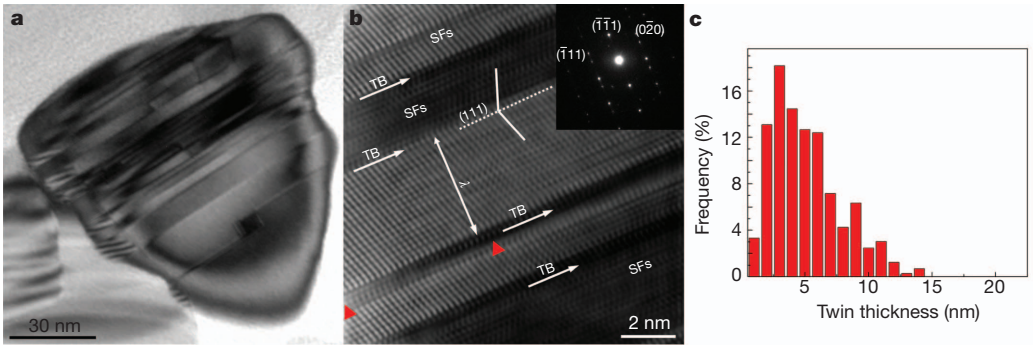

Figure 2 | Microstructure of synthetic nt-cBN. **a**, Bright-field TEM image of a nanograin. **b**, HRTEM image and corresponding selected area electron diffraction pattern (inset) along the [101] zone axis of the nanograin shown in **a**. Lamellar nanotwins with various thicknesses (λ) are present in the nanograin. The twinning plane is of the {111} type, and the lattice fringe angles across the twin plane are 70.53°. Stacking faults and Shockley dislocations (red triangles) are labelled. **c**, Thickness distribution of the twins measured from TEM and HRTEM images with an average twin thickness of 3.8 nm.

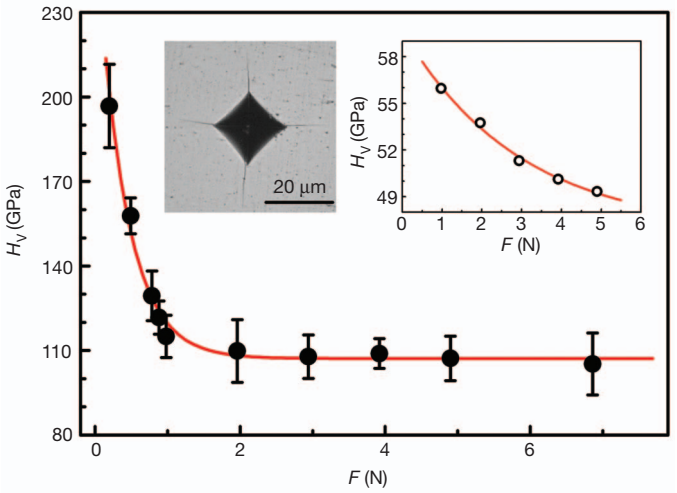

Figure 3 | The H_V of an nt-cBN bulk sample as a function of applied load (F). The H_V of the nt-cBN bulk decreases from ~196 GPa at 0.2 N to its asymptotic value, 108 GPa, beyond 3 N. Error bars indicate s.d. ($n = 5$). Left inset, an optical micrograph of the Vickers indentation with cracks produced at a load of 19.6 N. Right inset, the H_V–F curve of a 0.3-mm cBN single crystal. H_V does not reach its asymptotic value, and the crystal fractures when F exceeds 4.9 N.

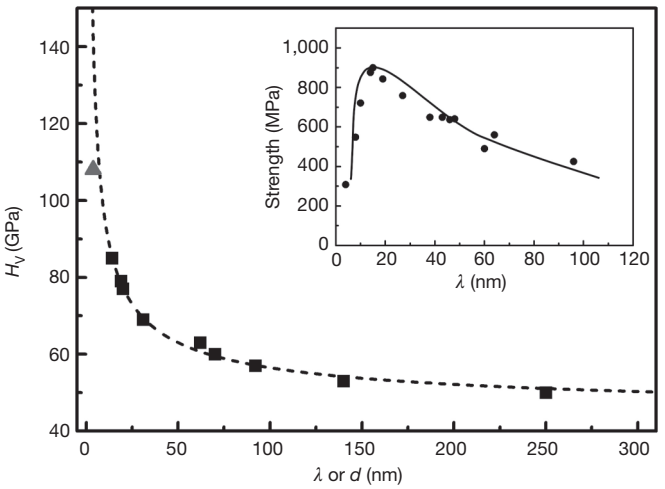

Figure 4 | H_V as a function of average grain size (d) or twin thickness (λ) for polycrystalline cBN bulk materials. Experimental data for nt-cBN bulk material (triangle) and for ng-cBN bulk materials[1] (squares) are shown. Using equation (1) to fit the experimental data, we obtained $H_V = 42.6 + 126d^{-1/2} + 130.7d^{-1}$. k (126 GPa nm$^{1/2}$) is taken from a previously reported value[1]. The fitted C (130.7 ± 16.8 GPa nm) parameter characterizing the quantum confinement effect is in excellent agreement with the theoretical value (136 GPa nm) from $211N_e^{1/3}\exp(-1.191f_i)$ for cBN. This coincidence is not accidental and may provide proof of the existence of the quantum confinement effect in the synthesized nt-cBN. Inset, the yield strength as a function of λ for nt-Cu, in which the critical λ is about 15 nm (ref. 15).

the applied load, respectively. The resulting K_{IC} reached a remarkably high value of 12.7 MPa m$^{1/2}$, which is about 4.5-fold that of cBN single crystal (2.8 MPa m$^{1/2}$) and almost twice that of micrometre-grain-sized cBN (6.8 MPa m$^{1/2}$) (ref. 2). This K_{IC} is 21% greater than that of ng-cBN (10.5 MPa m$^{1/2}$) (ref. 2) and 27% greater than the fracture toughness (10 MPa m$^{1/2}$) of commercial cemented tungsten carbide, a material widely used in the industry as a cutting tool[23].

The thermal stability of nt-cBN was characterized by using heat flow curves measured in air by differential scanning calorimetry (Supplementary Fig. 3). An onset oxidation temperature of ~1,294 °C was determined from the exothermic trough, which is higher than those of single-crystal cBN (~1,103 °C), ng-cBN (~1,187 °C) (ref. 2) and commercial polycrystalline cBN (~1,000 °C) (ref. 4). The high thermal stability of nt-cBN samples, apparently due to the nanotwinned structure, allows higher-temperature industrial applications.

Figure 4 shows that the hardness of polycrystalline cBN increases monotonically with decreasing microstructural size (grain size for grains and/or twin thickness for twins). On the basis of our recent theoretical model[20], the hardness dependence of the grain size (d) for cBN obeys

$$H_V = H_{HP} + H_{QC} = H_0 + kd^{-1/2} + Cd^{-1} \quad (1)$$

where H_{HP} ($= H_0 + kd^{-1/2}$) and H_{QC} ($= Cd^{-1}$) represent dislocation-related hardening based on the Hall–Petch effect[9,10] and bandgap-related hardening based on the speculated quantum confinement effect[24], respectively. H_0 is the single-crystal hardness and k is a material constant. C is a material-specific parameter equal to zero for metals, and equal to $211N_e^{1/3}\exp(-1.191f_i)$ for covalent materials[20], where N_e is the valence electron density and f_i is the Phillips ionicity of the chemical bond[25]. Both Hall–Petch and quantum confinement effects have been used to account for the hardening behaviour in ng-cBN with grain sizes down to 14 nm (ref. 1).

Our present results show that these two hardening mechanisms remain valid when the twin thickness is significantly reduced to 3.8 nm for cBN (Fig. 4). This finding on covalent cBN is in sharp contrast with those in metals, for which both yield strength and hardness decrease significantly (inset of Fig. 4) and the Hall–Petch hardening mechanism becomes invalid[14,15,26] when the twin thickness or grain size decreases to a critical value (typically ~10–15 nm). The continuously hardening behaviour with decreasing microstructural sizes (down to 3.8 nm) in cBN may be rationalized as follows. For nanotwins with thicknesses below 3.8 nm, the quantum confinement effect (which is inoperative in metals) becomes dominantly large according to equation (1) (see also the caption of Fig. 4). At a twin thickness of 3.8 nm, each twin lamella contains only about ten unit cells of cBN. This featured nanoscale geometry, as well as the very strong covalent B–N bonding, severely confines the migration of twin boundaries, which is known to induce hardness softening in nanotwinned metals[26].

The use of oBN nanoparticles as precursors is the key to synthesizing nt-cBN, and it highlights the important structural effects of spherical atomic arrangement in oBN on the formation of nanotwinned substructures. It has been established that coarse-grained graphite-like BN precursors can transform into grained cBN or wurtzite BN through martensitic transformation by means of puckering or buckling of the planar BN layers[3]. In our synthesis, the oBN precursors that we used contain naturally puckered BN layers (Fig. 1b), which make the transformation into cBN easier. The high concentration of puckered layers and defects (here, stacking faults; Fig. 1a) in oBN precursors provides ideal sites for the nucleation of cBN. Moreover, the specific orientation relations between coherent nucleus cBN and parent phase oBN must be reserved during the reconstructive phase transition[27]. As a result, multiple parallel laminated nanotwins form at the sub-grain level. High-density domain boundaries with ideal boundary structures in nanotwins make nt-cBN the most desirable superhard material yet achieved. This new material possesses the combined advantages of ultrahigh hardness, high thermal stability, and extremely high fracture toughness, providing a wide range of new industrial applications.

Our findings introduce a new strategy and direction in the quest for superhard materials. The synthesis of nanotwinned substructures by selecting suitable starting materials and optimal P–T conditions, and the use of hardening effects from interlocked nanotwins, are essential. On the basis of our results, if nanotwins at similar scales can be reproduced in polycrystalline diamond (isostructural to cBN and known for twinning in large crystals), an ultrahigh hardness exceeding that of ng-diamond would be achievable.

METHODS SUMMARY

Pure oBN nanospheres with diameters about 30–150 nm were synthesized with a chemical vapour deposition technique[28]. A schematic icosahedral model of a five-shell oBN nanoparticle was relaxed from the nested bucky onion of $B_{30}N_{30}$, $B_{120}N_{120}$, $B_{270}N_{270}$, $B_{480}N_{480}$ and $B_{750}N_{750}$ fullerenes. Geometric optimization was performed with the Forcite module of Materials Studio software, and the Universal Force Field was used. HPHT experiments were performed with a 10-MN two-stage large-volume multi-anvil system at Yanshan University, identical to that described in ref. 29. The standard COMPRES 10/5 sample assembly, consisting of a 10-mm spinel ($MgAl_2O_4$) octahedron with a Re heater and a $LaCrO_3$ thermal insulator, was used[30]. Temperature was measured *in situ* with Type C W-Re thermocouples, and pressures were estimated from previously obtained calibration curves at different temperatures[30]. Recovered bulk samples were about 2 mm in diameter and 0.2–0.5 mm in height. Microstructures of the bulks were characterized by TEM (JEOL-2010F) with an accelerating voltage of 200 kV at the University of New Mexico and TEM (JEM-2010) with an accelerating voltage of 200 kV at Yanshan University. Phase identification was performed with an X-ray powder diffractometer (D8 Discover) with Cu K_α radiation, and by Raman spectroscopy (Renishaw inVia). H_V and Knoop hardness (H_K) were measured with a microhardness tester (KB 5 BVZ). At least five hardness data points were taken for each load, and the hardness values were determined from the asymptotic-hardness region. Nanohardness (H_N) and Young's modulus (E) were measured with a Hysitron TI 950 TriboIndentor with Berkovich indenter at a peak load of 50 mN (see Supplementary Fig. 4 for details). Studies on oxidation resistance were performed in air by differential scanning calorimetry (NETZSCH STA 449 C) with a heating rate of 10 °C min^{-1} in the temperature range 20–1,500 °C.

Received 20 May; accepted 29 October 2012.

1. Dubrovinskaia, N. *et al.* Superhard nanocomposite of dense polymorphs of boron nitride: noncarbon material has reached diamond hardness. *Appl. Phys. Lett.* **90,** 101912 (2007).
2. Solozhenko, V. L., Kurakevych, O. O. & Le Godec, Y. Creation of nanostuctures by extreme conditions: high-pressure synthesis of ultrahard nanocrystalline cubic boron nitride. *Adv. Mater.* **24,** 1540–1544 (2012).
3. Britun, V. F. & Kurdyumov, A. V. Mechanisms of martensitic transformations in boron nitride and conditions of their development. *High Press. Res.* **17,** 101–111 (2000).
4. Sumiya, H., Uesaka, S. & Satoh, S. Mechanical properties of high purity polycrystalline cBN synthesized by direct conversion sintering method. *J. Mater. Sci.* **35,** 1181–1186 (2000).
5. Dub, S. N. & Petrusha, I. A. Mechanical properties of polycrystalline cBN obtained from pyrolytic gBN by direct transformation technique. *High Press. Res.* **26,** 71–77 (2006).
6. Wentorf, R. H., DeVries, R. C. & Bundy, F. P. Sintered superhard materials. *Science* **208,** 873–880 (1980).
7. Liew, W. Y. H., Yuan, S. & Ngoi, B. K. A. Evaluation of machining performance of STAVAX with PCBN tools. *Int. J. Adv. Manuf. Technol.* **23,** 11–19 (2004).
8. Krauss, A. R. *et al.* Ultrananocrystalline diamond thin films for MEMS and moving mechanical assembly devices. *Diamond Related Materials* **10,** 1952–1961 (2001).
9. Hall, E. O. The deformation and ageing of mild steel: III. Discussion of results. *Proc. Phys. Soc. B* **64,** 747–753 (1951).
10. Petch, N. J. The cleavage strength of polycrystals. *J. Iron Steel Inst.* **174,** 25–28 (1953).
11. Irifune, T., Kurio, A., Sakamoto, S., Inoue, T. & Sumiya, H. Ultrahard polycrystalline diamond from graphite. *Nature* **421,** 599–600 (2003).
12. Sumiya, H. & Irifune, T. Hardness and deformation microstructures of nano-polycrystalline diamonds synthesized from various carbons under high pressure and high temperature. *J. Mater. Res.* **22,** 2345–2351 (2007).
13. Schiøtz, J., Di Tolla, F. D. & Jacobsen, K. W. Softening of nanocrystalline metals at very small grain sizes. *Nature* **391,** 561–563 (1998).
14. Schiøtz, J. & Jacobsen, K. W. A maximum in the strength of nanocrystalline copper. *Science* **301,** 1357–1359 (2003).
15. Lu, L., Chen, X., Huang, X. & Lu, K. Revealing the maximum strength in nanotwinned copper. *Science* **323,** 607–610 (2009).
16. Pande, C. S. & Cooper, K. P. Nanomechanics of Hall–Petch relationship in nanocrystalline materials. *Prog. Mater. Sci.* **54,** 689–706 (2009).
17. He, L. L., Akaishi, M. & Horiuchi, S. Structural evolution in boron nitrides during the hexagonal–cubic phase transition under high pressure at high temperature. *Microsc. Res. Tech.* **40,** 243–250 (1998).
18. Oku, T., Hiraga, K., Matsuda, T., Hirai, T. & Hirabayashi, M. Twin structures of rhombohedral and cubic boron nitride prepared by chemical vapor deposition method. *Diamond Related Materials* **12,** 1138–1145 (2003).
19. Brazhkin, V. *et al.* What does 'harder than diamond' mean? *Nature Mater.* **3,** 576–577 (2004).
20. Tian, Y., Xu, B. & Zhao, Z. Microscopic theory of hardness and design of novel superhard crystals. *Int. J. Refract. Met. Hard Mater.* **33,** 93–106 (2012).
21. Harris, T. K., Brookes, E. J. & Taylor, C. J. The effect of temperature on the hardness of polycrystalline cubic boron nitride cutting tool materials. *Int. J. Refract. Met. Hard Mater.* **22,** 105–110 (2004).
22. Solozhenko, V. L., Dub, S. N. & Novikov, N. V. Mechanical properties of cubic BC_2N, a new superhard phase. *Diamond Related Materials* **10,** 2228–2231 (2001).
23. Berger, C., Scheerer, H. & Ellermeier, J. Modern materials for forming and cutting tools—overview. *Materialwiss. Werkstofftech.* **41,** 5–17 (2010).
24. Tse, J. S., Klug, D. D. & Gao, F. M. Hardness of nanocrystalline diamonds. *Phys. Rev. B* **73,** 140102 (2006).
25. Gao, F. M. *et al.* Hardness of covalent crystals. *Phys. Rev. Lett.* **91,** 015502 (2003).
26. Li, X., Wei, Y., Lu, L., Lu, K. & Gao, H. Dislocation nucleation governed softening and maximum strength in nano-twinned metals. *Nature* **464,** 877–880 (2010).
27. Oleinik, G. S., Petrusha, I. A., Danilenko, N. V., Kotko, A. V. & Shevchenko, S. A. Crystal-oriented mechanism of dynamic recrystallization nucleation in cubic boron nitride. *Diamond Related Materials* **7,** 1684–1692 (1998).
28. Tang, C. C., Bando, Y., Huang, Y., Zhi, C. Y. & Golberg, D. Synthetic routes and formation mechanisms of spherical boron nitride nanoparticles. *Adv. Funct. Mater.* **18,** 3653–3661 (2008).
29. Wang, Y. *et al.* The large-volume high-pressure facility at GSECARS: a 'Swiss-army-knife' approach to synchrotron-based experimental studies. *Phys. Earth Planet. Inter.* **174,** 270–281 (2009).
30. Leinenweber, K. D. *et al.* Cell assemblies for reproducible multi-anvil experiments (the COMPRES assemblies). *Am. Mineral.* **97,** 353–368 (2012).

Supplementary Information is available in the online version of the paper.

Acknowledgements We thank J. K. Yu for help with the differential scanning calorimetry measurements. Y.J.T. and Z.Y.L. acknowledge financial support from the Ministry of Science and Technology of China (grants 2011CB808205 and 2010CB731605), Y.J.T., D.L.Y., Y.M.M. and J.L.H. are grateful for financial support from the National Natural Science Foundation of China (grants 51121061, 51172197, 11025418 and 91022029), and Y.B.W. acknowledges financial support from the US National Science Foundation (EAR-0968456).

Author Contributions Y.J.T. conceived the project. Y.J.T., B.X., D.L.Y. and Y.B.W. designed the experiments. C.C.T. synthesized oBN precursors, Y.J.T., B.X., D.L.Y., Y.B.W., Y.F.G., K.L. and Z.S.Z. performed the HPHT experiments, Y.B.J. and W.T.H. performed TEM observations, and B.W. performed molecular dynamics simulations. Y.J.T., B.X., D.L.Y., Y.M.M., Y.B.W., L.-M.W., J.L.H. and Z.Y.L. analysed the data. Y.J.T., B.X., Y.M.M. and Y.B.W. co-wrote the paper. Y.J.T., B.X. and D.L.Y. contributed equally to the study. All authors discussed the results and commented on the manuscript.

Author Information Reprints and permissions information is available at www.nature.com/reprints. The authors declare no competing financial interests. Readers are welcome to comment on the online version of the paper. Correspondence and requests for materials should be addressed to Y.J.T. (fhcl@ysu.edu.cn).